chemosensors

*Article*

# Electrochemical Multiplexed N-Terminal Natriuretic Peptide and Cortisol Detection in Human Artificial Saliva: Heart Failure Biomedical Application

**El Kahina Ghedir [1], Abdoullatif Baraket [2,*], Messaoud Benounis [1], Nadia Zine [2] and Abdelhamid Errachid [2,*]**

[1] Laboratory of Sensors, Instrumentations and Process (LCIP), Institute of Science and Technology, University of Khenchela, Route de El Hamma, Khenchela 40000, Algeria; ghedir@hotmail.fr (E.K.G.); benounis@yahoo.fr (M.B.)
[2] Institute de Sciences Analytiques (ISA), Université de Lyon—UMR 5280, 5 rue de la Doua, 69100 Villeurbanne, France; nadia.zine@univ-lyon1.fr
* Correspondence: a.baraket@gmail.com (A.B.); abdelhamid.errachid-el-salhi@univ-lyon1.fr (A.E.)

**Abstract:** The early detection at low concentration, by non-invasive methods, of cardiac biomarkers in physiological fluids has attracted the interest of researchers over the last decade. This enables early diagnosis and prediction of the first signs of heart failure (HF). In this respect, the analysis of human saliva remains the most suitable medium for this non-invasive approach, as it contains a highly interesting biological matrix for general health and disease monitoring. In this work, we developed a highly sensitive multiplexed immunosensor for direct simultaneous detection of both N-terminal Natriuretic Peptide (NT-proBNP) and Cortisol in human artificial saliva (AS). The developed biosensor platform based on silicon nitride substrate was composed from four gold working microelectrodes (WEs) and an integrated counter and reference microelectrode. Gold WEs were biofunctionalized through carboxyl diazonium (4-APA) to immobilize both anti-NT-proBNP and anti-Cortisol antibodies for simultaneous detection. The electroaddressing of the 4-APA onto the gold WE surfaces was realized with cyclic voltammetry (CV), while the interaction between antibodies and antigens in PBS was monitored using electrochemical impedance spectroscopy (EIS). The antigen detection in human AS was realized with EIS combined with the standard addition method. The immunosensor was highly sensitive and selective toward the corresponding biomarkers in both PBS and artificial human saliva as well as in the presence of other potential interfering biomarkers such as tumor necrosis factor alpha (TNF-α) and interleukin-10 (IL-10). The limit of detection (LOD) was at 0.2 pg/mL for NT-proBNP within the range of 0.03 to 0.9 pg/mL, while the LOD for Cortisol was 0.06 ng/mL within the range of 0.02 to 0.6 ng/mL for Cortisol in artificial saliva. The developed immunosensor is very promising for significant detection in physiological media, and time reducing as it allows the simultaneous detection of various biomarkers.

**Keywords:** multiplexed detection; N-terminal brain natriuretic peptide; cortisol; human saliva analysis; electrochemical impedance spectroscopy; heart failure



**Citation:** Ghedir, E.K.; Baraket, A.; Benounis, M.; Zine, N.; Errachid, A. Electrochemical Multiplexed N-Terminal Natriuretic Peptide and Cortisol Detection in Human Artificial Saliva: Heart Failure Biomedical Application. *Chemosensors* **2023**, *11*, 416. https://doi.org/10.3390/chemosensors11070416

Academic Editor: Alina Vasilescu

Received: 14 May 2023
Revised: 20 July 2023
Accepted: 20 July 2023
Published: 24 July 2023



## 1. Introduction

Heart failure (HF) is amongst the most rapidly increasing causes of death around the world, particularly for the elderly [1,2]. HF is a complex clinical syndrome caused by a wide range of structural or functional abnormalities of the heart which result in the impairment of the heart's ability to fill or to pump out blood, thus failing to deliver oxygen at a rate commensurate with the requirements to organs and tissues [3,4]. HF is identified by symptoms such as a swelling of the legs and ankles, high jugular venous pressure, extreme fatigue, and intolerance to exercise; all these symptoms combine to provide very poor quality of life for patients with HF [5]. However, the clinical diagnosis of HF based only on these nonspecific signs and symptoms is a big challenge, which may entail delays

in accurate diagnosis and treatment, thus worsening clinical outcomes and increasing healthcare costs [3].

Due to all these reasons, the early diagnosis of HF and cardiac dysfunction is extremely important to avoid complications of the patient's health. For this reason, several HF biomarkers circulating in plasma, serum, blood or saliva have been taken into account for early HF diagnosis [6–10]. The standard techniques for the detection of these cardiac biomarkers were based on Enzyme-Linked Immuno-Sorbent Assay (ELISA) [11,12] and electrochemiluminescence immunoassay (ECLIA) [13,14]. Although these techniques are standard and accurate, they still have some limitations, such as the requirement for specialized personnel and laboratories, and expensive instruments and reagents, as well as a long detection time.

In order to overcome these problems, numerous biosensors and immunosensors have been developed in the literature in the last two decades to detect these cardiac biomarkers at low concentrations [15–22]. Most of these biosensors were based on the detection of a single biomarker at a time, which is time consuming. However, biosensors based on multiplexed detection could be an alternative solution which allow for accurate detection of different cardiac biomarkers at the same time [23–25].

The detection of cardiac biomarkers in saliva offers several advantages when compared to blood, e.g., they be easily and unobtrusively collected, even from critical subjects (e.g., children, the elderly, and disabled people) [26]. Recently Barhoumi et al. and Bellagambi et al. have reported respectively the detection of TNF-α based on chronoamperometric and impedimetric biosensors in human saliva at 1 pg/mL [18]) and 3.1 pg/mL [20]. These cytokines are considered characteristic of HF with complementary clinical data [27,28].

Another interesting cardiac biomarker, Amino N-terminal pro-brain natriuretic peptide (NT-proBNP), which is one of the families of peptidic hormones, was identified as a standard biomarker for HF [7,29–32]. Indeed, this biomarker was identified as the gold standard biomarker of HF by both European and American guidelines as increased plasma levels of circulating NT-proBNP in patients with congestive HF are directly related to the severity of congestive heart failure [33]. NT-proBNP was detected at 0.4 ng/mL in human plasma [34] and at 1 pg/mL in saliva [33] with the ELISA technique. Generally, NT-proBNP is detected in the literature using standard techniques such as ELISA. NT-proBNP was detected at 0.58 nM in human serum by using a biosensor, as reported by [35]. Here, the authors used an electrochemical biosensor based on metalloimmunoassay on a paper electrode platform.

On the other hand, Cortisol, "the stress hormone", is also considered a promising biomarker of HF, since the correlation between oxidative stress and HF has been demonstrated [36–38]. In contrast to NT-proBNP, many biosensors have been developed in the literature for Cortisol detection. This latter was detected at 10 ng/mL in human serum and blood [39], and at 0.05 ng/mL in human saliva [40].

In this work, we describe the development of an electrochemical immunosensor platform based on silicon substrate for the simultaneous detection of both NT-proBNP and Cortisol in artificial human saliva. Monoclonal antibodies (mAb) anti-NT-proBNP and monoclonal antibodies (mAb) anti-Cortisol were immobilized onto gold WEs through functionalization with 4-Aminophenylacetic acid (4-APA) (carboxyl diazonium). Cyclic voltammetry (CV) was applied for the biofunctionalization and the characterization of gold WE surface properties, while electrochemical impedance spectroscopy (EIS) combined with the standard addition method was used to quantify NT-proBNP and Cortisol antigens in artificial human saliva [20,21,28].

## 2. Materials and Methods

### *2.1. Chemicals and Reagents*

4-Aminophenylacetic acid (4-carboxymethylaniline) (4-APA), from Acros Organics (France), sodium nitrite ($NaNO_2$), hydrochloricacid (HCl) 37%, pure ethanol, ethanolamine, phosphate-buffered saline (PBS) tablets, potassium hexacyanoferrate (III) ($K_3Fe(CN)_6$), and

potassium hexacyanoferrate (II) trihydrate ($K_4Fe(CN)_6 \cdot 3H_2O$), sodium phosphate dibasic ($Na_2HPO_4$, PharmaGrade), anhydrous Calcium chloride ($CaCl_2$), Sodium chloride (NaCl), sodium hydrogen carbonate ($NaHCO_3$), mucin, and urea were purchased from Sigma Aldrich (France). N-(3-dimethylaminopropyl)-N-ethyl-carbodiimidehydrochloride (EDC), N-hydroxy-succinimide (NHS), Monoclonal Antibody anti NT-Pro-BNP (mAb-NT-proBNP, Cat. No.4NT1cc-24E11CC), and NT-proBNP antigene (Cat.No.8NT2) were purchased from HyTst (Finland). Monoclonal Antibody anti-Cortisol (mAb-Cortisol, XM210) and Hydrocortisone (ab141250) were purchased from Abcam (Cambridge, United Kingdom). Recombinant Human IL-10 (1064-IL) and Tumor necrosis factor TNF-α (210-TA) were purchased from R&D Systems (Lille, France). Millipore Milli-Q nanopure water (resistivity >18 MΩ cm) was produced by a Millipore ReagentWater System (Molsheim, France). The PBS buffer used in this study was prepared by dissolving PBS tablets in the nanopure water as indicated by the supplier, at pH 7.4.

### *2.2. Preparation of Antibodies and Biomarker Standard Solutions*

Anti-Cortisol antibodies were reconstituted according to the protocol provided by the supplier; each aliquot contained 10 µL with a concentration of 2 mg/mL. This latter was stored at −20 °C until use. For anti-NT-proBNP antibodies, the mother solution with a concentration of 6.1 mg/mL was stored as received at 4 °C until use.

Before each analysis, a solution of 10 µg/mL of mAb-anti-Cortisol and mAb-anti-NT-proBNP was prepared respectively by diluting the appropriate amount of stock solution in PBS containing 0.09% sodium azide.

Biomarkers were prepared at different concentrations. Firstly, Cortisol antigen was dissolved in ethanol at 1 mg/mL, and then used to prepare standard solutions at different concentrations by diluting the appropriate amount of the stock solution in PBS. NT-proBNP was aliquoted (10 µL at 1.2 mg/mL) then stored at −80 °C until use. Biomarker standard solutions were prepared by mixing NT-proBNP and Cortisol before electrochemical analyses.

Similarly, the standard solutions containing the possible interferences (IL-10 and TNF-α) were prepared in PBS. All the standard solutions were prepared by weighing.

### *2.3. Sample Preparation*

Human artificial saliva (AS) was prepared as described by [20,41] and stored at 4 °C until use. Then, appropriate amounts of NT-proBNP and Cortisol stock solution were diluted in AS at different concentrations (0.03, 0.06, 0.1, 0.3, 0.6, and 0.9 pg/mL) and (0.02, 0.04, 0.1, 0.2, 0.4, and 0.6 ng/mL) for NT-proBNP and Cortisol, respectively (Table 1).

**Table 1.** NT-proBNP and Cortisol concentrations for each level.

| Levels | NT-proBNP (pg/mL) | Cortisol (ng/mL) | IL-10 (pg/mL) | TNF-α (pg/mL) |
|---|---|---|---|---|
| 1 | 0.03 | 0.02 | 0.03 | 0.03 |
| 2 | 0.06 | 0.04 | 0.06 | 0.06 |
| 3 | 0.1 | 0.1 | 0.1 | 0.1 |
| 4 | 0.3 | 0.2 | 0.3 | 0.3 |
| 5 | 0.6 | 0.4 | 0.6 | 0.6 |
| 6 | 0.9 | 0.6 | 0.9 | 0.9 |

For the standard addition method (SAM), a mixture containing 100 pg/mL of NT-proBNP and 100 ng/mL of Cortisol was prepared in human AS to simulate an unknown sample to be analyzed by SAM. Then, a volume constant of 50 µL of the unknown sample was added to each of four volumetric flasks of 1 mL capacity. Afterwards, 950 µL of PBS was added to the first flask (Level 0) to reach the final volume of 1 mL. Then, the unknown sample was added with increasing volumes (50, 100, 150 µL) to each of the three remaining flasks. This corresponds to addition of 5 pg/mL–5 ng/mL (Level 1), 10 pg/mL–10 ng/mL (Level 2), and 15 pg/mL–15 ng/mL (Level 3) of both NT-proBNP and Cortisol to the

subsequent flasks. Finally, the three remaining flasks were made up to volume (1 mL) with PBS.

### *2.4. Bio-Functionalization of Gold WEs*

The biosensor platform is made of four gold working electrodes (WE), two silver and silver chloride Ag/AgCl reference electrodes (REs), and one platinum counter electrode (CE), as shown in Figure 1. The biosensor platform functionalization has been previously described by Ghedir et al. [19]. Briefly, before the chemical surface functionalization of gold WEs, the device was pre-cleaned with sonication in acetone, followed by rinsing with ethanol and deionized water, and was then placed into a UV/O3 to remove all organic contaminants and to ensure a clean gold surface.

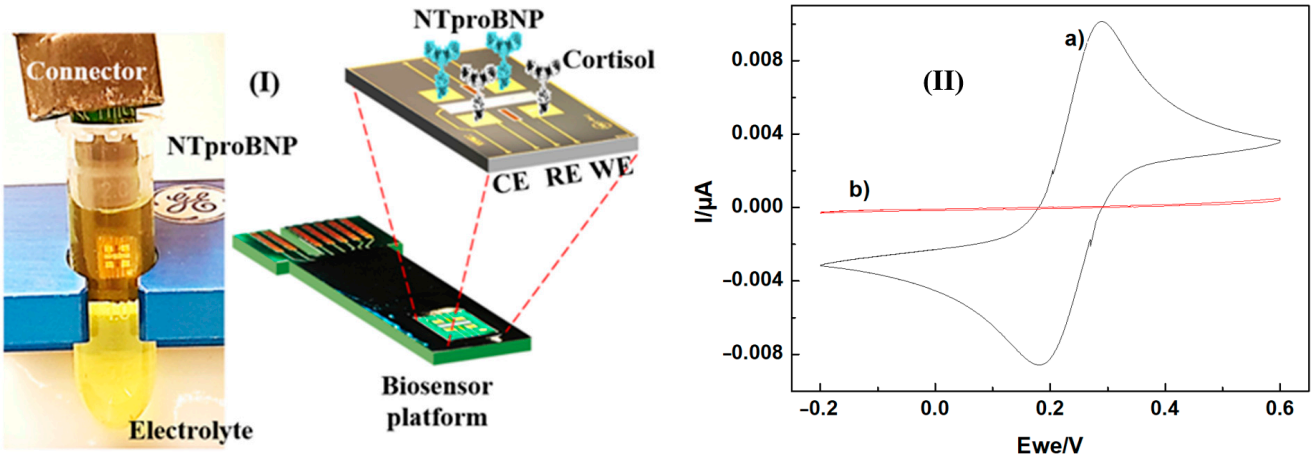


**Figure 1.** (**I**) Electrochemical biosensor platform connected to the potentiostat and dropped in the ferric electrolyte solution. (**II**) Cyclic voltammogram before (a) and after gold WE functionalization with 4-APA (b) an important decrease in peak-to-peak of the CV cycle was observed after 4-APA deposition, due to the decrease in the electron transfer rate created by the 4-APA blocking layer.

Subsequently, 4-APA molecules were electrochemically deposited onto only two gold WEs using the cyclic voltammetry (CV) technique as described in [20,21]. Indeed, 3 mM of 4-APA solution was prepared in water with 10 mM of HCl and 10 mM $NaNO_2$ in ice. The device was placed into this solution and only two WEs were connected to the potentiostat. Then, fifteen CV cycles were applied within the potential range of 0 V to −1.1 V vs. Ag/AgCl RE at the scan rate of 80 mV/s.

The biosensor platform was then abundantly rinsed with deionized water and dried with a stream of nitrogen. The terminal carboxylic acid (–COOH) groups of 4-APA were activated in an ethanolic solution of EDC (0.4 M)/NHS (0.1 M) for 1 h at room temperature (22 ± 2 °C). Afterwards, the activated gold WE surfaces were rapidly washed with 0.1 M HCl and immediately incubated for 1 h in 30 µL of PBS containing anti-NT-proBNP mAb at 4 °C. This step was fundamental to ensure the covalent bonding of the amine terminal groups on the antibody and the activated –COOH from 4-APA. Finally, the WEs were rinsed with PBS to remove the unbonded antibodies and the remaining active carboxylic acid groups were deactivated by incubation in 0.1% ethanolamine solution for 20 min at 4 °C. This step is crucial to prevent nonspecific bonding during the detection process. The same procedure was repeated for the two other gold WEs to immobilize anti-Cortisol antibodies.

### *2.5. Electrochemical Measurements*

All electrochemical measurements were carried out at room temperature (22 ± 2 °C) in a Faraday box using an VMP3 potentiostat (BioLogic Science Instruments, Claix, France) monitored by EC-Lab soft-ware (version 11.30, BioLogic Science Instruments, France).

Gold WEs were characterized before and after functionalization by dropping the biosensor platform in ferric electrolyte (5 mM $K_3[Fe(CN)_6]/K_4[Fe(CN)_6]$ in PBS solution). CV characterization was optimized at 80 mV/s, and the switching potential was scanned between −0.2 to 0.6 V.

The simultaneous detection of NTproBNP and Cortisol was carried out by using EIS measurements in both standard solutions and human AS with concentrations in the range of 0.03 pg/mL to 0.9 pg/mL and 0.02 ng/mL to 0.6 ng/mL, respectively. EIS potential was fixed at 0.228 V versus Ag/AgCl reference electrode, over a range of frequencies from 100 mHz to 10 kHz, using a modulation voltage of 80 mV [21].

## 3. Results and Discussion

### *3.1. Cyclic Voltammetry*

The biosensor platform (sizes 7 × 4 mm) based on silicon substrate and integrating four gold WE, CE, and RE was sealed onto the PCB board (Figure 1I). The fabrication process was previously detailed by Baraket et al. [21]. The biosensor was connected to the potentiostat and dropped in 1.5 mL of ferric electrolyte (Supplementary Figure S1).

Figure 1IIa shows the visible Fe (II)/Fe (III) redox peaks corresponding to CV measurements of bare gold WEs. However, an important decrease in peak-to-peak of the CV cycle was observed after 4-APA deposition, due to the decrease in the electron transfer rate created by the 4-APA blocking layer (Figure 1IIb).

### *3.2. Detection of NTptoBNP and Cortisol*

#### 3.2.1. Detection in PBS

Prior to simultaneous detection, we first studied the detection of the biomarkers NT-proBNP and corticole separately. Here, we dedicated a single biosensor platform to each biomarker. Figure 2a shows the Nyquist diagram of NT-proBNP detection. The first Nyquist plot curve (-■-) corresponds to the functionalized biosensor with mAb-anti-NT-proBNP in the absence of the corresponding biomarkers. After the first incubation of the biosensor in a solution containing 0.03 pg/mL of NT-proBNP, the Nyquist plot curves (-●-) shifted from the first. By increasing the concentration of NT-proBNP, the Nyquist plot semi-circles continued to increase, thus showing the detection phenomenon.

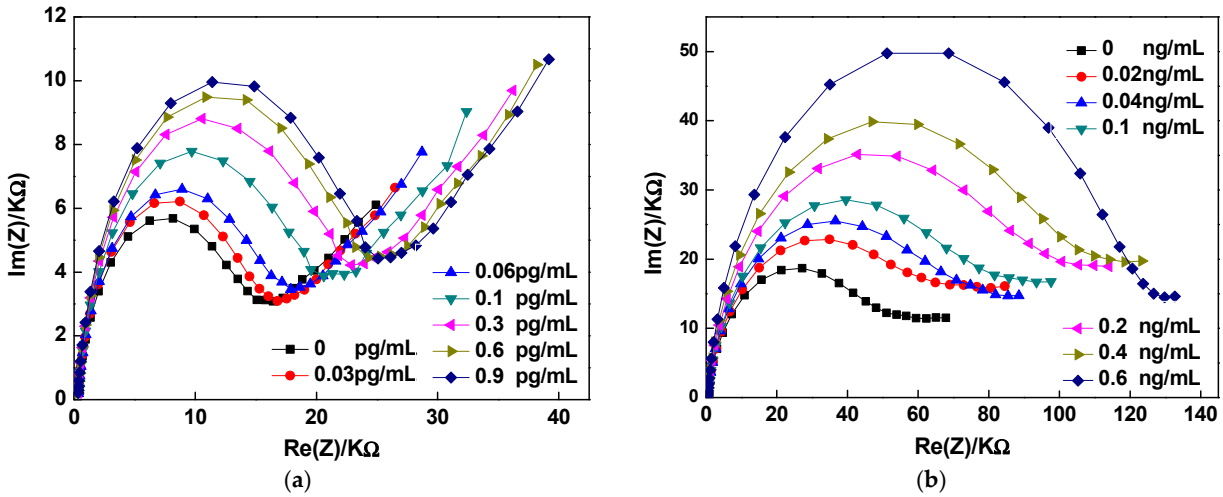


**Figure 2.** *Cont.*

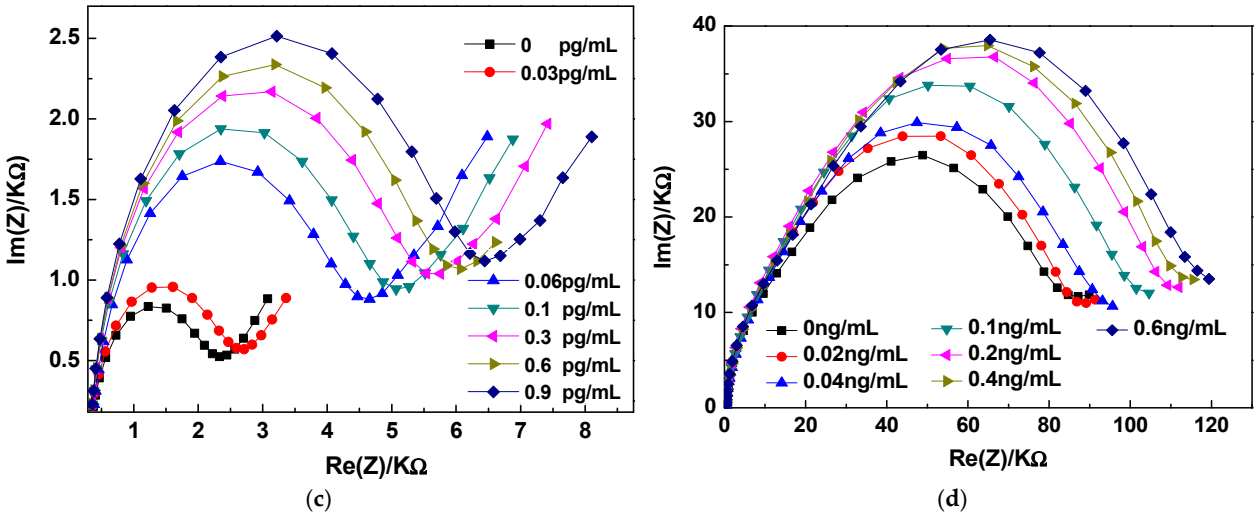


**Figure 2.** Nyquist plots of impedance (Zr vs. Zi: at 5 mM of $K_3[Fe(CN)_6]/K_4[Fe(CN)_6]$ in PBS pH 7.4 solution) at: (**a**) various NT-proBNP concentrations without Cortisol, (**b**) various Cortisol concentrations without NT-proBNP, (**c**) various NT-proBNP concentrations in the presence of Cortisol, (**d**) various Cortisol concentrations in the presence of NT-proBNP.

The same behavior was observed for the other biosensor platform dedicated to Cortisol detection (Figure 2b).

After having detected the antigens separately, the biosensor was used for simultaneous detection by functionalizing two Wes with NT-proBNP and the other two Wes with Cortisol as described in the experiment section. Then, the same EIS experimental procedure used previously was repeated for simultaneous detection. Figure 2c,d show the Nyquist plot curves corresponding to the simultaneous detection of both NT-proBNP and Cortisol, respectively. Here, the first curves of both Nyquist plots (-■-) correspond to the functionalized biosensor with mAb-anti-NT-proBNP and mAb-anti-Cortisol in the absence of the two corresponding biomarkers. After the first incubation of the biosensor in a solution containing 0.03 pg/mL of NT-proBNP and 0.02 ng/mL of Cortisol, the Nyquist plots curves (-●-) have shifted from the first, thus showing the simultaneous detection of both NT-proBNP and Cortisol. Afterwards, the biosensor platform was rinsed abundantly with PBS in order to prevent nonspecific adsorption and incubated again in PBS solution containing the next concentrations of NT-proBNP and Cortisol. By increasing the concentration of these proteins, the Nyquist plot curves continued to increase, thus showing the sensitivity of the biosensor to detect NT-proBNP and Cortisol simultaneously.

All these Nyquist plot semi-circles were fitted using the Randles equivalent circuit (Supplementary Figure S2) [21]. The normalized data were presented as a function of the variation in charge transfer resistant Rct using the relation: ΔRct/Rct (where ΔRct = Rct (biomarkers)—Rct (antibodies)/Rct(antibodies)) as a function of NT-proBNP and Cortisol concentrations, respectively (Figure 3). These concentration levels are summarized in Table 1.

As can be observed from Figure 3a,b, for both single and simultaneous detection, the biosensor platform demonstrated a high sensitivity toward the corresponding biomarkers without any interference between NT-proBNP and cortisol.

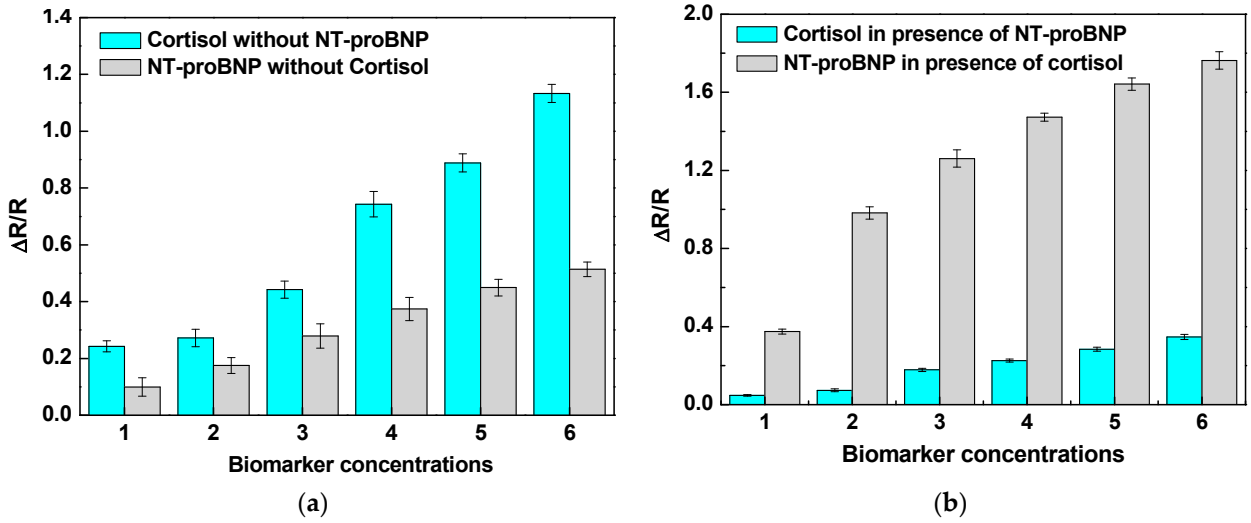


**Figure 3.** (**a**) Sensitivity of the biosensor for NT-proBNP and Cortisol detection using one biosensor for each biomarker, (**b**) sensitivity of the biosensor for NT-proBNP and Cortisol detection using only one biosensor for both biomarkers.

3.2.2. Simultaneous Detection with Interferences in PBS

In order to study the selectivity of this biosensor, the same simultaneous detection experience was repeated by adding other potential interferents like TNF-α and IL-10 in addition to NT-proBNP and Cortisol. Figure 4 shows the high selectivity and sensitivity of the biosensor toward the corresponding biomarkers NT-proBNP and Cortisol in the presence of the other interferents.

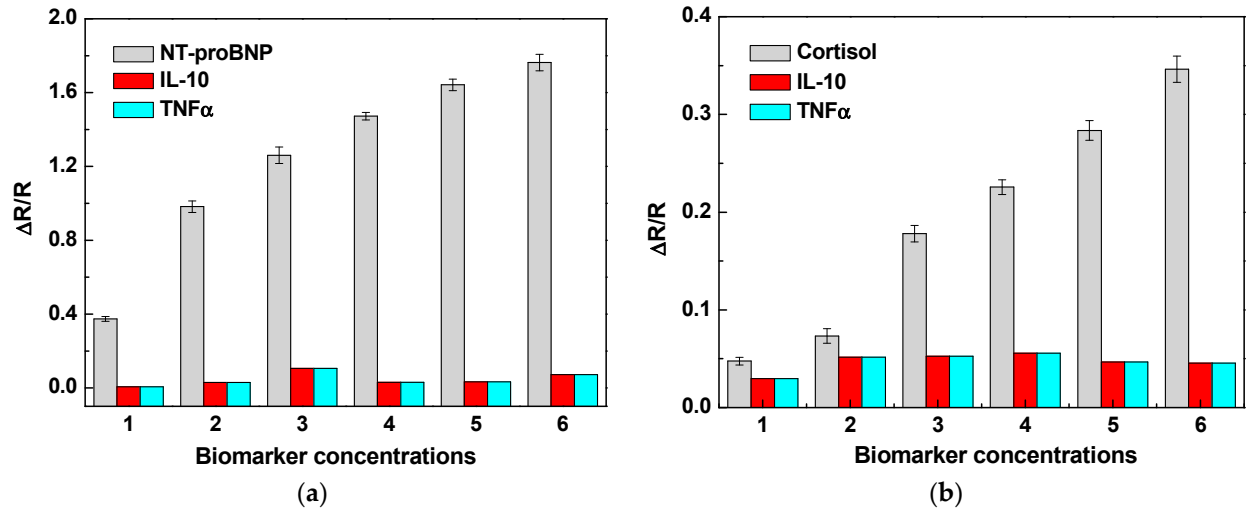


**Figure 4.** (**a**) Sensitivity of the biosensor functionalized with Ab-anti-Cortisol for the detection of Cortisol, IL-10, and TNF-α. (**b**) Sensitivity of the biosensor functionalized with Ab-anti-NT-proBNP for the detection of NT-proBNP, IL-10 and TNF-α in PBS.

Two linear segments with different slopes for the concentration of each biomarker, NT-proBNP and Cortisol, were observed (Figure 4a,b). For NT-proBNP and within the range of 0.03 to 0.1 pg/mL (Level 1 to 3), the regression equation was $Y = 13.95X - 0.045$, ($R^2 = 0.99$) and from 0.1 to 0.9pg/mL (Level 1 to 6), the regression equation was $Y = 0.066X + 1.2$, ($R^2 = 0.96$). For Cortisol, from 0.02 to 0.1 ng/mL (Level 1 to 3), the regression equation was $Y = 1.84X + 0.006$, ($R^2 = 0.9$), and from 0.1 to 0.6 ng/mL (Level 3 to 6), the regression equation was $Y = 0.33X + 0.15$, ($R^2 = 0.98$). The detection of limit (LOD) was calculated

by using the formula 3*Standard deviation/Slope [42], and was found at 0.07 pg/mL and 0.06 ng/mL for NT-proBNP and Cortisol, respectively.

#### 3.2.3. Simultaneous Detection in AS

In order to further explore the performance of the biosensor, it was used for simultaneous detection in human AS. Here, the biosensor was subject to successive incubations in human AS, instead of PBS, with increasing concentrations of the corresponding biomarkers NT-proBNP and Cortisol. The biosensor was rinsed abundantly after each incubation and characterized with EIS.

As can be observed from Figure 5a,b, and similar to the previous EIS experiment, a shift between the first (-■-) and the second (-●-) Nyquist plot curves was observed after the first incubation of the biosensor in human AS containing 0.03 pg/mL of NT-proBNP and 0.02 ng/mL of Cortisol. By increasing the concentration of these biomarkers, the Nyquist plot curves continued to increase thus showing the sensitivity of the biosensor. However, here the shift between Nyquist plot semi-circles was much higher when compared to the detection in PBS. This shift does not completely correspond to NT-proBNP and Cortisol detection; however, it was attributed to the nonspecific adsorption phenomena due to the matrix effect of AS [43].

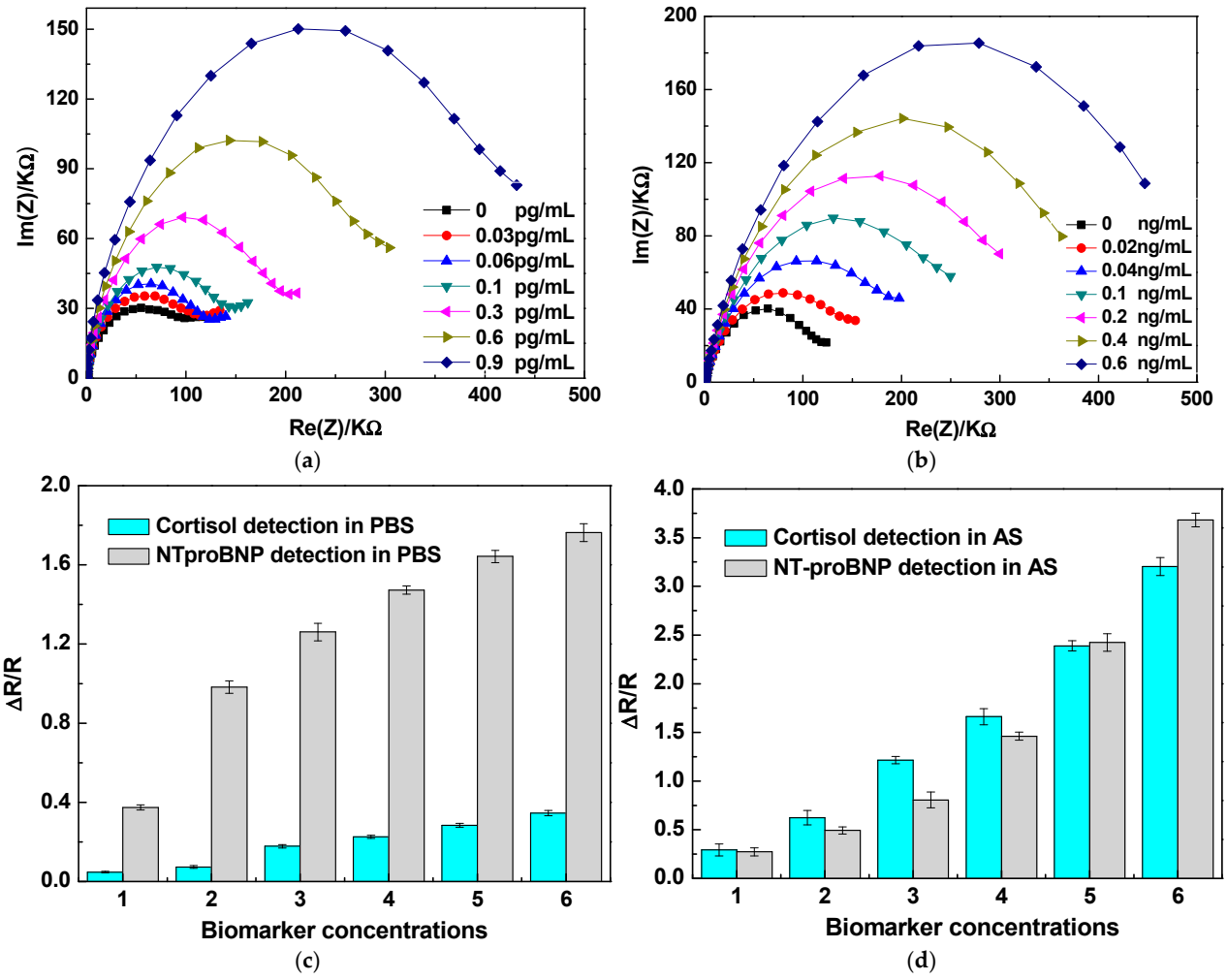


**Figure 5.** Simultaneous responses of the biosensor at mixtures containing different concentrations of (**a**) NT-proBNP and (**b**) Cortisol in AS. Sensitivity of the biosensor for NT-proBNP and Cortisol detection: (**c**) in PBS (**d**) in human AS.

The normalized data ΔRct/Rct are presented in Figure 5d. Here, the biosensor showed the same behavior of sensitivity that we observed in PBS Figure 5c.

To find out if this sensitivity in AS corresponds in part to the biomarker detection or just to the matrix effect of human AS, the selectivity of the biosensor was investigated. Here, the same previous EIS experimental procedure was repeated by analyzing standard solutions with increasing concentrations of NT-proBNP and Cortisol in AS in the presence of potential interferents.

Figure 6 shows clearly that the biosensor was highly sensitive toward the corresponding biomarkers NT-proBNP and Cortisol when compared to the interferents IL-10 and TNF-α. This demonstrates the ability of the biosensor to specifically detect the corresponding biomarkers within a complex physiological medium like human AS. Here, the biosensor kept the same previous behaviors by showing two linear areas, even in a complex physiological medium. Indeed, for NT-proBNP, from 0.03 to 0.1 pg/mL, the regression equation was Y = 6.19X + 0.09, ($R^2$= 0.99) and from 0.1 to 0.9 pg/mL, the regression equation was Y = 3.09X + 0.338, ($R^2$ = 0.89). For Cortisol, from 0.02 to 0.1ng/mL, the regression equation was Y = 11.16X + 0.08, ($R^2$ = 0.99), and from 0.1 to 0.6.ng/mL it was at Y = 3.46X + 0.85, ($R^2$ = 0.99). The LOD in human AS was calculated using the same previous formula and was found to be 0.2 pg/mL for NT-proBNP and 0.06 ng/mL for Cortisol.

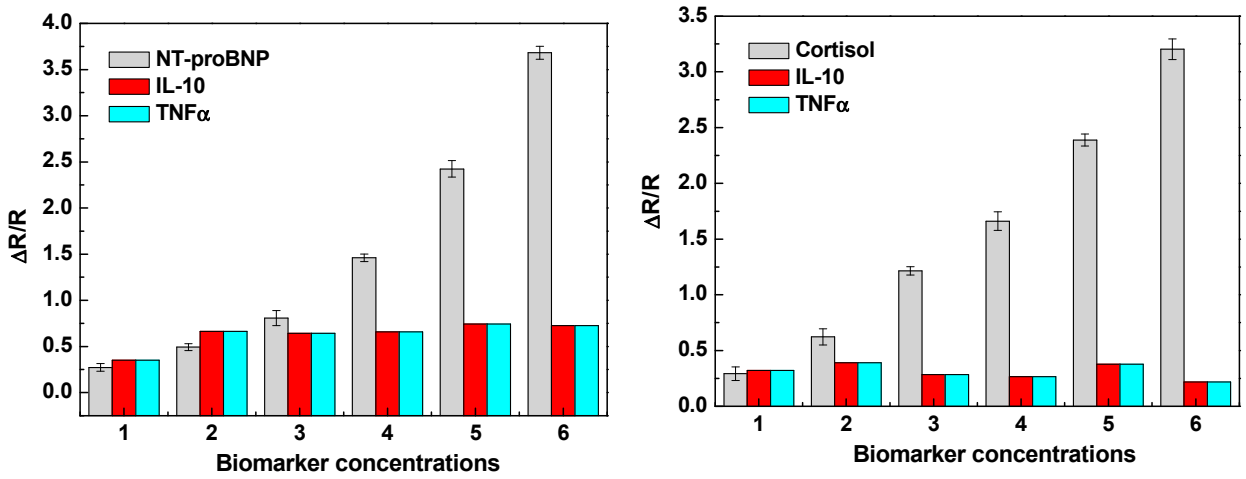


(**a**) (**b**)

**Figure 6.** Sensitivity of the biosensor for the detection of (**a**) NT-proBNP and (**b**) Cortisol in the presence of IL-10 and TNF-α in AS.

### 3.2.4. Detection in Artificial Saliva Using the Standard Addition Method

The standard addition method combined with EIS [20] was used to simulate the simultaneous detection of NT-proBNP and Cortisol in human AS using an unknown sample, as described in Section 2.3. Here, the unknown sample was prepared in AS with 100 pg/mL of NT-proBNP and 100 ng/mL of Cortisol, and these concentrations should be found using the standard addition method. Figure 7 shows the EIS analyses for the detection of both NT-proBNP and Cortisol. The first Nyquist plot corresponds to Level 0, which contains only 50µL of the unknown sample in PBS. By increasing the concentration of NT-proBNP and Cortisol in Level 1, Level 2, and Level 3, the Nyquist plot semi-circles continue to increase, thus showing the detection of the corresponding biomarkers.

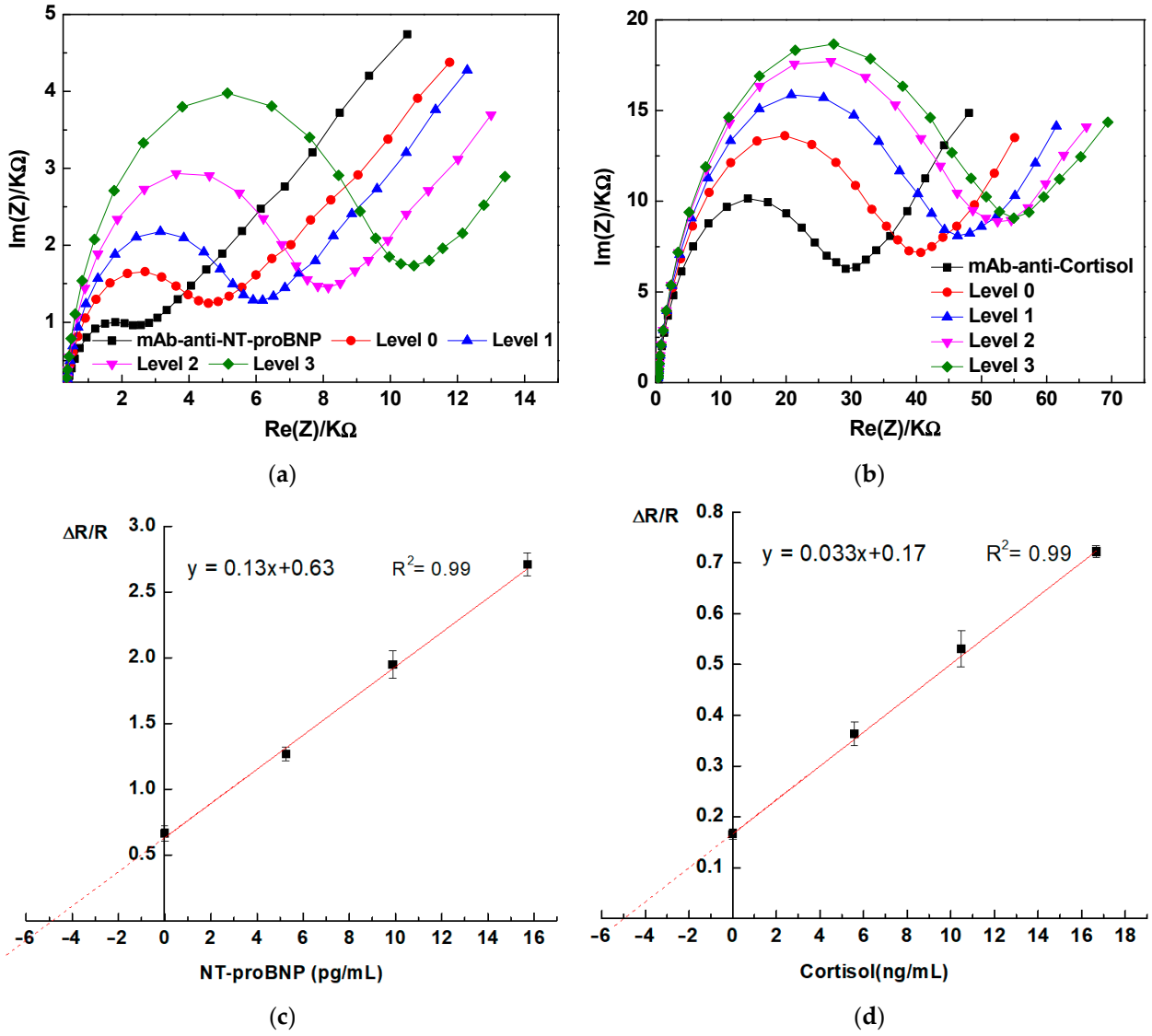


**Figure 7.** Nyquist impedance plots (Zr vs. Zi: at 5 mM of $K_3[Fe(CN)_6]/K_4[Fe(CN)_6]$ in PBS pH 7.4 solution) obtained from the standard addition method performed on artificial saliva: (**a**) Level 1 (corresponding to an addition of 0 pg/mL), Level 2 (addition of 5 pg/mL), Level 3 (addition of 10 pg/mL), Level 4 (addition of 15 ng/mL) of NT-proBNP. (**b**) Level 1 (corresponding to an addition of 0 ng/mL), Level 2 (addition of 5 ng/mL), Level 3 (addition of 10 ng/mL), and Level 4 (addition of 15 ng/mL) of Cortisol. (**c**) Sensitivity curve used to calculate the concentration of analyte in the unknown sample for NT-proBNP and (**d**) sensitivity curve used to calculate the concentration of analyte in the unknown sample for Cortisol. The intersection of the extrapolation of the linear curve (red line) with the axis concentrations corresponded to the unknown sample concentration of both NT-proBNP and cortisol.

After data normalization, a linear relationship between the Rct variation and NT-proBNP and Cortisol concentrations was found Figure 7c,d. The linear equations after data fitting were Y = 0.13X + 0.63 ($R^2$ = 0.99) and Y = 0.033X + 0.17 ($R^2$ = 0.99) for NT-proBNP and Cortisol respectively.

The standard addition method consists of using the linear equation curve to extrapolate the intercept value on the negative abscissa axis. Here, the intersection of the extrapolation of the linear curve with the axis concentrations corresponded to the unknown sample concentration (Level 0) which was found at 4.85 pg/mL and 4.97 ng/mL for NT-proBNP and Cortisol respectively.

These concentrations correspond to the unknown sample (Level 0), and by considering the dilution factor used to prepare Level 0 (in this case 20 times dilution), the concentration of the mother solution was 97 pg/mL and 99.58 ng/mL for NT-proBNP and Cortisol respectively. These concentrations are close to the 100 pg-ng/mL prepared previously to simulate the unknown sample.

## 4. Conclusions

A highly sensitive multiplexed immunosensor for simultaneous NT-proBNP and Cortisol detection in human artificial saliva was described in this work. The established biosensor based on gold working microelectrodes (WEs) was biofunctionalized through carboxyl diazonium to immobilize anti-NT-proBNP and anti-Cortisol antibodies. The immunosensor demonstrated a good sensitivity in a critical range from 0.03 to 0.9 pg/mL and 0.02 to 0.6 ng/mL for both NT-proBNP and Cortisol, respectively. No cross detection was observed between NT-proBNP and Cortisol, and the biosensor showed a good selectivity in the presence of other potential interferents (IL-10 and TNF-α). The biosensor platform is very promising and can save time by simultaneously detecting NT-proBNP and Cortisol in complex physiological medium and with a small amount of sample.

On the other hand, C-E Karachaliou et al. [44] recently reported an exhaustive study about the detection of Cortisol in different physiological serums, and particularly in human saliva. Here, the author has mentioned the selectivity of immunosensors toward cortisol in the presence of other steroids when compared to other analytical immunoassays. However, although the biosensor developed in this study did demonstrate better sensitivity with a significant LOD of both cortisol and NT-proBNP in the presence of other potential interferences such as IL-10 and TNF-α, which are present in patients suffering from cardiovascular disease, it is necessary to study in the future also the selectivity in the presence of other interferents like steroids to ensure that the results of cortisol and NT-proBNP quantification are as accurate as possible.

The main aim of this study was the development of an immunosensor for the detection of biomarkers in physiological media. However, it is necessary to mention the challenge of automation of manufacturing and detection processes. Indeed, although the developed biosensor in this study did demonstrate better detection and selectivity, it remains at this stage limited by the number of manual steps required for its calibration. This latter is necessary so that the clinician can in the future take only a single measurement and project it onto the sensor's calibration curve to measure the biomarkers' quantity in the saliva of HF patients. In this regard, work is in progress in our laboratory to miniaturize the pententiostat for on-site measurements and to develop a mobile phone application connected to the miniaturized potentiostat to facilitate measurements by clinicians. This is fully in line with the current trend towards continuous and real-time monitoring of cortisol and NT-proBNP levels for rapid diagnosis using biosensors. These electrochemical biosensors are easily miniaturized [21,22], enabling reduced analysis costs with fast response times, rapid and continuous measurements, and much lower use of reagents. This will have a beneficial impact on the health of patients and on the economy through the early detection of the first signs of inflammation and the reduction in the budget of hospitals.

**Supplementary Materials:** The following supporting information can be downloaded at: https://www.mdpi.com/article/10.3390/chemosensors11070416/s1, Figure S1: (A) Electrochemical biosensor platform sealed onto the PCB board using an epoxy resin (Epo-Tek H70E-2LC, from Epoxy Technology) and the microelectrode pads wire-bonded to the gold tracks of the BCP using aluminum wire (25 µm Ø) (Kulicke&Soffa 4523A). (B) The bonding area of the device, the bonding wires, and the gold tracks of the PCB were encapsulated using the same resin (Epo-Tek H70E-2LC) to protect them from the electrolyte solution. (C) The biosensor is based on silicon substrate sizes 7 × 4 mm and contains four gold WE, two RE, and central platinum CE. (D) The biosensor is dropped in 1.5 mL of ferric electrolyte solution and connected to the potentiostat through shielded cable to avoid all electrical noises. Figure S2: Randles equivalent circuit used for Nyquist plot semi-circles fitting, where Rs represents the electrolyte resistance, Rct is the charge-transfer resistance, W is Warburg impedance, and Q1 the constant phase element, an equivalent model of the double-layer capacitance.

**Author Contributions:** Writing—original draft preparation, formal analysis, methodology, validation, E.K.G.; Writing, editing, formal analysis, validation, A.B.; Validation M.B.; formal analysis, supervision N.Z.; review, editing and supervision, A.E. All authors have read and agreed to the published version of the manuscript.

**Funding:** The authors acknowledge the financial support from POC4 allergies project (Grant Agreement No. 768686), which received funding from ERA PerMed ERA-NET, and the financial support from Bionanosens project (Grant agreement No. 951887), which received funding from the European Union's Horizon 2020. The authors would also like to thank the Algerian–French B+ Scholarship Program (PROFAS B+) for its support in funding this work.

**Institutional Review Board Statement:** Not applicable.

**Informed Consent Statement:** Not applicable.

**Data Availability Statement:** The data that support the findings of this study are available from the corresponding author upon reasonable request.

**Conflicts of Interest:** The authors declare no conflict of interest.

## References

1. Benjamin, E.J.; Muntner, P.; Alonso, A.; Bittencourt, M.S.; Callaway, C.W.; Carson, A.P.; Chamberlain, A.M.; Chang, A.R.; Cheng, S.; Das, S.R.; et al. Heart disease and stroke Statistics-2019 update a report from the American Heart Association. *Circulation* **2019**, *139*, e56–e528. [CrossRef] [PubMed]
2. Virani, S.S.; Alonso, A.; Benjamin, E.J.; Bittencourt, M.S.; Callaway, C.W.; Carson, A.P.; Chamberlain, A.M.; Chang, A.R.; Cheng, S.; Delling, F.N.; et al. Heart disease and stroke statistics—2020 update: A report from the American Heart Association. *Circulation* **2020**, *141*, E139–E596. [CrossRef] [PubMed]
3. Kurmani, S.; Squire, I. Acute heart failure: Definition, classification and epidemiology. *Curr. Heart Fail. Rep.* **2017**, *14*, 385–392. [CrossRef] [PubMed]
4. Lee, K.S.; Moser, D.K.; Dracup, K. Relationship between self-care and comprehensive understanding of heart failure and its signs and symptoms. *Eur. J. Cardiovasc. Nurs.* **2018**, *17*, 496–504. [CrossRef]
5. Riley, J.P.; Beattie, J.M. Palliative care in heart failure: Facts and numbers. *ESC Heart Fail.* **2017**, *4*, 81–87. [CrossRef]
6. Suthahar, N.; Meems, L.M.; Ho, J.E.; de Boer, R.A. Sex-related differences in contemporary biomarkers for heart failure: A review. *Eur. J. Heart Fail.* **2020**, *22*, 775–788. [CrossRef]
7. Sarhene, M.; Wang, Y.; Wei, J.; Huang, Y.; Li, M.; Li, L.; Acheampong, E.; Zhengcan, Z.; Xiaoyan, Q.; Yunsheng, X.; et al. Biomarkers in heart failure: The past, current and future. *Heart Fail. Rev.* **2019**, *24*, 867–903. [CrossRef]
8. Berezin, A.E. Circulating biomarkers in heart failure. In *Heart Failure: From Research to Clinical Practice*; Springer: Berlin/Heidelberg, Germany, 2018; pp. 89–108.
9. Stanciu, A.E. Cytokines in heart failure. In *Advances in Clinical Chemistry*; Elsevier: Amsterdam, The Netherlands, 2019; pp. 63–113.
10. Gohel, V.; Jones, J.A.; Wehler, C.J. Salivary biomarkers and cardiovascular disease: A systematic review. *Clin. Chem. Lab. Med. (CCLM)* **2018**, *56*, 1432–1442. [CrossRef]
11. Saenger, A.K.; Rodriguez-Fraga, O.; Ler, R.; Ordonez-Llanos, J.; Jaffe, A.S.; Goetze, J.P.; Apple, F.S. Specificity of B-Type Natriuretic Peptide Assays: Cross-Reactivity with Different BNP, NT-proBNP, and proBNP Peptides. *Clin. Chem.* **2017**, *63*, 351–358. [CrossRef]
12. Kavsak, P.A.; Lam, C.S.P.; Saenger, A.K.; Jaffe, A.S.; Collinson, P.; Pulkki, K.; Omland, T.; Lefèvre, G.; Body, R.; Ordonez-Llanos, J.; et al. Educational Recommendations on Selected Analytical and Clinical Aspects of Natriuretic Peptides with a Focus on Heart Failure: A Report from the IFCC Committee on Clinical Applications of Cardiac Bio-Markers. *Clin. Chem.* **2019**, *65*, 1221–1227. [CrossRef]
13. Aberle, J.; Zur Wiesch, C.S.; Flitsch, J.; Veigel, J.; Schön, G.; Jung, R.; Lautenbach, A.; Rotermund, R.; Riedel, N. Specificity of late-night salivary cortisol measured by automated electrochemiluminescence immunoassay for Cushing's disease in an obese population. *J. Endocrinol. Investig.* **2018**, *41*, 1325–1331. [CrossRef]
14. Dong, X.; Zhao, G.; Li, X.; Miao, J.; Fang, J.; Wei, Q.; Cao, W. Electrochemiluminescence immunoassay for the N-terminal pro-B-type natriuretic peptide based on resonance energy transfer between a self-enhanced luminophore composed of silver nanocubes on gold nanoparticles and a metal-organic framework of type MIL-125. *Microchim. Acta* **2019**, *186*, 811. [CrossRef]
15. Nessark, F.; Eissa, M.; Baraket, A.; Zine, N.; Nessark, B.; Zouaoui, A.; Bausells, J.; Errachid, A. Capacitance Polypyrrole-based Impedimetric Immunosensor for Interleukin-10 Cytokine Detection. *Electroanalysis* **2020**, *32*, 1795–1806. [CrossRef]
16. Halima, H.B.; Zine, N.; Gallardo-González, J.; El Aissari, A.; Sigaud, M.; Alcacer, A.; Bausells, J.; Errachid, A. A Novel Cortisol Biosensor Based on the Capacitive Structure of Hafnium Oxide: Application for Heart Failure Monitoring. In Proceedings of the 2019 20th International Conference on Solid-State Sensors, Actuators and Microsystems & Eurosensors XXXIII (TRANSDUCERS & EUROSENSORS XXXIII), Berlin, Germany, 23–27 June 2019; pp. 1067–1070.

17. Barhoumi, L.; Bellagambi, F.G.; Vivaldi, F.M.; Baraket, A.; Clément, Y.; Zine, N.; Ali, M.B.; Elaissari, A.; Errachid, A. Ultrasensitive immunosensor array for TNF-α detection in artificial saliva using polymer-coated magnetic microparticles onto screen-printed gold electrode. *Sensors* **2019**, *19*, 692. [CrossRef]
18. Barhoumi, L.; Baraket, A.; Bellagambi, F.G.; Karanasiou, G.S.; Ali, M.B.; Fotiadis, D.I.; Bausells, J.; Zine, N.; Sigaud, M.; Errachid, A. A novel chronoamperometric immunosensor for rapid detection of TNF-α in human saliva. *Sens. Actuators B Chem.* **2018**, *266*, 477–484. [CrossRef]
19. Ghedir, E.; Baraket, A.; Kouchar, S.; Rabai, S.; Benounis, M.; Alcacer, A.; Streklas, A.; Bausells, J.; Zine, N.; Jaffrezic, N.; et al. Electrochemical Immunosensor for NT-proBNP Detection in Artificial Human Saliva: Heart Failure Biomedical Application. *Proceedings* **2018**, *2*, 1085.
20. Bellagambi, F.G.; Baraket, A.; Longo, A.; Vatteroni, M.; Zine, N.; Bausells, J.; Fuoco, R.; Di Francesco, F.; Salvo, P.; Karanasiou, G.S.; et al. Electrochemical biosensor platform for TNF-α cytokines detection in both artificial and human saliva: Heart failure. *Sens. Actuators B Chem.* **2017**, *251*, 1026–1033. [CrossRef]
21. Baraket, A.; Lee, M.; Zine, N.; Sigaud, M.; Bausells, J.; Errachid, A. A fully integrated electrochemical biosensor platform fabrication process for cytokines detection. *Biosens. Bioelectron.* **2017**, *93*, 170–175. [CrossRef]
22. Baraket, A.; Lee, M.; Zine, N.; Yaakoubi, N.; Bausells, J.; Errachid, A. A flexible electrochemical micro lab-on-chip: Application to the detection of interleukin-10. *Microchim. Acta* **2016**, *183*, 2155–2162. [CrossRef]
23. Sinha, A.; Tai, T.-Y.; Li, K.-H.; Gopinathan, P.; Chung, Y.-D.; Sarangadharan, I.; Ma, H.-P.; Huang, P.-C.; Shiesh, S.-C.; Wang, Y.-L.; et al. An integrated microfluidic system with field-effect-transistor sensor arrays for detecting multiple cardiovascular biomarkers from clinical samples. *Biosens. Bioelectron.* **2019**, *129*, 155–163. [CrossRef] [PubMed]
24. Zhao, J.; Du, J.; Luo, J.; Chen, S.; Yuan, R. A novel potential-resolved electrochemiluminescence immunosensor for the simultaneous determination of brain natriuretic peptide and cardiac troponin I. *Sens. Actuators B Chem.* **2020**, *311*, 127934. [CrossRef]
25. Lee, J.-K.; Wang, I.; Huang, C.-H.; Chen, Y.-F.; Huang, N.-T.; Lin, C.-T. Pre-Clinical Tests of an Integrated CMOS Biomolecular Sensor for Cardiac Diseases Diagnosis. *Sensors* **2017**, *17*, 2733. [CrossRef] [PubMed]
26. Bellagambi, F.G.; Lomonaco, T.; Salvo, P.; Vivaldi, F.; Hangouët, M.; Ghimenti, S.; Biagini, D.; Di Francesco, F.; Fuoco, R.; Errachid, A. Saliva sampling: Methods and devices. An overview. *TrAC Trends Anal. Chem.* **2020**, *124*, 115781. [CrossRef]
27. Shirazi, L.F.; Bissett, J.; Romeo, F.; Mehta, J.L. Role of inflammation in heart failure. *Curr. Atheroscler. Rep.* **2017**, *19*, 27. [CrossRef] [PubMed]
28. Bartekova, M.; Radosinska, J.; Jelemensky, M.; Dhalla, N.S. Role of cytokines and inflammation in heart function during health and disease. *Heart Fail. Rev.* **2018**, *23*, 733–758. [CrossRef]
29. Wang, X.-Y.; Zhang, F.; Zhang, C.; Zheng, L.-R.; Yang, J. The Biomarkers for Acute Myocardial Infarction and Heart Failure. *BioMed Res. Int.* **2020**, *2020*, 2018035. [CrossRef]
30. Szunerits, S.; Mishyn, V.; Grabowska, I.; Boukherroub, R. Electrochemical cardiovascular platforms: Current state of the art and beyond. *Biosens. Bioelectron.* **2019**, *131*, 287–298. [CrossRef]
31. Ibrahim, N.E.; Januzzi, J.L., Jr. Established and emerging roles of biomarkers in heart failure. *Circ. Res.* **2018**, *123*, 614–629. [CrossRef]
32. Matsuo, A.; Nagai-Okatani, C.; Nishigori, M.; Kangawa, K.; Minamino, N. Natriuretic peptides in human heart: Novel insight into their molecular forms, functions, and diagnostic use. *Peptides* **2019**, *111*, 3–17. [CrossRef]
33. Bellagambi, F.G.; Petersen, C.; Salvo, P.; Ghimenti, S.; Franzini, M.; Biagini, D.; Hangouët, M.; Trivella, M.G.; Di Francesco, F.; Paolocchi, A.; et al. Determination and stability of N-terminal pro-brain natriuretic peptide in saliva samples for monitoring heart failure. *Sci. Rep.* **2021**, *11*, 13088. [CrossRef]
34. Colom, G.; Salvador, J.-P.; Acosta, G.; Albericio, F.; Royo, M.; Marco, M.-P. Competitive ELISA for N-terminal pro-brain natriuretic peptide (NT-proBNP) determination in human plasma. *Analyst* **2020**, *145*, 6719–6727. [CrossRef] [PubMed]
35. Pollok, N.E.; Rabin, C.; Walgama, C.T.; Smith, L.; Richards, I.; Crooks, R.M. Electrochemical detection of NT-proBNP using a metalloimmunoassay on a paper electrode platform. *ACS Sens.* **2020**, *5*, 853–860. [CrossRef] [PubMed]
36. Zea, M.; Bellagambi, F.G.; Halima, H.B.; Zine, N.; Jaffrezic-Renault, N.; Villa, R.; Gabriel, G.; Errachid, A. Electrochemical sensors for cortisol detections: Almost there. *TrAC Trends Anal. Chem.* **2020**, *132*, 116058. [CrossRef]
37. Grimm, G.; Resl, M.; Heinisch, B.B.; Hülsmann, M.; Luger, A.; Clodi, M.; Vila, G. B-type natriuretic peptide increases cortisol and catecholamine concentrations in healthy subjects. *J. Appl. Physiol.* **2017**, *122*, 1249–1254. [CrossRef]
38. Singh, R.B.; Isaza, A.; Wilczynska, A.; Kartikey, K.; Kareem, Z.; Alshihaby, W.; Almansory, A.; Hadi, N.R.; Bassm, M.; View Point. Cortisol and the Heart. *World Heart J.* **2019**, *11*, 73–77.
39. Upasham, S.; Tanak, A.; Jagannath, B.; Prasad, S. Development of ultra-low volume, multi-bio fluid, cortisol sensing platform. *Sci. Rep.* **2018**, *8*, 16745. [CrossRef]
40. Uygun, H.D.E.; Uygun, Z.O.; Canbay, E.; Sağın, F.G.; Sezer, E. Non-invasive cortisol detection in saliva by using molecularly cortisol imprinted fullerene-acrylamide modified screen printed electrodes. *Talanta* **2020**, *206*, 120225. [CrossRef]
41. Tlili, C.; Myung, N.V.; Shetty VMulchandani, A. Label-free, chemiresistor immunosensor for stress biomarker cortisol in saliva. *Biosens. Bioelectron.* **2011**, *26*, 4382–4386. [CrossRef] [PubMed]
42. Swartz, M.E.; Krull, I.S. *Analytical Method Development and Validation*; CRC Press: Boca Raton, FL, USA, 2018.

43. Baraket, A.; Lee, M.; Zine, N.; Caruso, R.; Trivella, M.; Errachid, A. Electrochemical Biosensor for Interleukin-10 Detection in Real Human Plasma Patients: Heart Failure Biomedical Application. *Int. J. Cardiovasc. Res.* **2016**, *6*, 1. [CrossRef]
44. Karachaliou, C.-E.; Koukouvinos, G.; Goustouridis, D.; Raptis, I.; Kakabakos, S.; Petrou, P.; Livaniou, E. Cortisol Immunosensors: A Literature Review. *Biosensors* **2023**, *13*, 285. [CrossRef]